Influence of thermal annealing on the perpendicular magnetic anisotropy of Pt/Co/AlOx trilayers

B. Rodmacq,[1] A. Manchon,[1,2] C. Ducruet,[1] S. Auffret,[1] and B. Dieny[1]
[1]*SPINTEC, URA 2512 CEA/CNRS, 38054 Grenoble Cedex 9, France*
[2]*Department of Physics, University of Arizona, Tucson, Arizona 85721, USA*
(Received 6 June 2008; revised manuscript received 17 November 2008; published 22 January 2009)

The influence of thermal annealing on Pt/Co/AlOx trilayers has been investigated up to 450 °C as a function of the plasma oxidation time of the AlOx layer. Both magnetic properties of the Co layer and transport properties are strongly modified upon annealing. The perpendicular magnetic anisotropy reaches very large values, while the Hall angle increases with annealing temperature. This study reveals that this trilayer system possesses tunable magnetic anisotropy properties, which can be controlled by varying either oxidation time or annealing temperature. These results are compared with those obtained on standard Pt/Co/Pt trilayers which show, on the contrary, a continuous degradation of their magnetic properties upon annealing.

DOI: 10.1103/PhysRevB.79.024423 PACS number(s): 75.70.Cn, 75.30.Gw, 73.40.Rw, 73.43.Qt

I. INTRODUCTION

Spin-dependent tunneling in magnetic tunnel junctions[1] (MTJs) is one of the most exciting issues in spin electronics that may lead to very important applications, such as magnetic read-heads,[2] or magnetic random access memories.[3] MTJs are usually composed of two ferromagnetic layers separated by a metallic oxide barrier like AlOx (Ref. 4) or MgO.[5] In such systems, the tunneling transport is governed by the spin-dependent interfacial densities of states, as well as the electronic states within the barrier.[6] Consequently, the homogeneity of the insulator and the quality of its interfaces deeply influence the transport properties of the MTJ.

Shortly after the observation of large room-temperature tunneling magnetoresistance[4] (TMR) in AlOx-based magnetic tunnel junctions, Sousa *et al.*[7] demonstrated that thermal annealing at about 250 °C could greatly improve the transport properties of magnetic tunnel junctions. It was indeed understood that the initial oxidation of a Co/Al bilayer is quite inhomogeneous. When the Al surface is exposed to oxygen, the oxygen atoms preferably migrate along the Al grain boundaries and even penetrate into the grain boundaries of the Co underlying electrode.[8] Then upon annealing, thermally activated diffusion of oxygen atoms into the aluminum grains takes place, leading to a more homogeneous tunnel barrier and to a reduction in interfacial roughness. However, for higher annealing temperatures (300 °C), thermal migration of the metallic atoms seems to reduce the ability of the tunnel barrier to filter the electron spin and to deteriorate the ferromagnetic electrodes.[9–11]

The case of MgO-based magnetic tunnel junctions[5] is slightly different since the crystallization of the tunnel barrier as well as that of the amorphous ferromagnetic CoFeB electrodes seem to be crucial to obtain a high TMR ratio. Then, the maximum of TMR is obtained for annealing temperature of the order of 350–500 °C.[12,13]

Recently, we demonstrated that plasma or natural oxidation of an AlOx-based tunnel barrier has a significant influence on the magnetic anisotropy properties of a Pt/Co/AlOx trilayer.[14] For an optimal oxidation time (in the case of plasma oxidation of an Al layer of a given thickness), the Co/AlOx interface is fully oxidized, whereas the oxygen atoms have not yet penetrated into the Co layer (in other words, all Co-Al bondings are replaced by Co-O bondings). In this situation, the presence of a substantial amount of oxygen atoms at this interface induces a strong perpendicular magnetic anisotropy (PMA) which overcomes the in-plane anisotropy of the Co layer.

PMA has been studied both experimentally[15,16] and theoretically[17] and can be understood based on Bruno's theory.[18] In the case of Co/AlOx interface, the $3d_{z^2}$ orbital of Co hybridizes with the $2p$ orbitals of oxygen. This hybridization lowers the Co-O binding energy, perpendicularly to the interface. As a consequence, the orbitals perpendicular to the interface possess a lower energy than the orbitals lying in the plane (related to the parameter Δ in Ref. 18), creating a strong perpendicular magnetic anisotropy despite the relatively weak spin-orbit coupling.

The study presented in Ref. 14 revealed that a range of optimal oxidation conditions exists to obtain fully oxidized Co/AlOx interface. Under these conditions, the magnetization of the thin Co layer ($\approx$0.6 nm) lies out of plane, forming a single domain structure. This effect is quite general since it has been observed for different Pt/Co/MOx trilayers (M=Mg, Al, Ta, Ru, Cr, etc.).[14,19,20] Moreover, preliminary investigations have recently shown that, for underoxidized trilayers with in-plane magnetic anisotropy, high-temperature annealing could also lead to the appearance of a strong perpendicular magnetic anisotropy.[21]

The influence of annealing on the perpendicular magnetic anisotropy of the trilayer presents a significant interest from different points of view. First, it allows the control of the oxidation process in MTJs through PMA measurements, without microfabrication. Second, the presence of a sizable interfacial magnetic anisotropy may be extremely interesting for designing MTJs (Ref. 22) with magnetization perpendicular to the interfaces. Up to now, a number of solutions have been proposed to grow perpendicular MTJs, such as $L1_0$ PtCo electrodes,[23] TbCoFe electrodes,[24] Co/Pd (Ref. 25) or Co/Pt (Refs. 26 and 27) multilayers. From this point of view, the achievement of high interfacial PMA together with high interfacial spin-polarization at Co/AlOx interface is of great interest. Finally, from a more fundamental perspective, the influence of interfacial orbital anisotropy on tunneling

properties of MTJs has recently been studied both theoretically and experimentally.[28] The appearance of orbital anisotropy at the interface between the barrier and the ferromagnetic electrode creates an interfacial spin-orbit interaction that can strongly influence the interfacial densities of states.

In this paper, we study the influence of thermal annealing (up to 450 °C) of Pt/Co/AlOx samples, in which the metallic Al layer has been plasma oxidized for different times. The magnetic properties (perpendicular magnetic anisotropy and nucleation field) as well as transport properties (Hall angle) appear to be deeply influenced by this annealing process. Large values of PMA and Hall angle are obtained, depending on the annealing temperature and on the oxidation time, making these samples very interesting for both conventional and perpendicular MTJ, extraordinary Hall-effect (EHE) sensors applications and anisotropic TMR studies.

This paper is organized as follows: Section II presents the magnetic properties of the samples before annealing. The influence of thermal annealing on the above mentioned properties is described in Sec. III. A general interpretation is given in Sec. IV, based on our previous x-ray spectroscopic studies presented in Refs. 14 and 21. Finally, in Sec. V, we compare these results to those obtained on classical Pt/Co/Pt trilayers.

II. MAGNETIC PROPERTIES IN THE AS-DEPOSITED STATE

Pt(3 nm)/Co(0.6 nm)/Al(1.6 nm) trilayers were deposited onto thermally oxidized silicon substrates by conventional dc magnetron sputtering with a base pressure of 10^{-8} mbar and with typical deposition rates of 0.05 nm/s (for Co and Al) to 0.1 nm/s (for Pt). Samples were then transferred under vacuum in a separate treatment chamber and oxidized using an oxygen rf plasma with a partial pressure of 3×10^{-3} mbar and a power of 10 W during an oxidation time t varying between 15 and 60 s.

Annealing was performed in a high-vacuum furnace for 30 min at different temperatures up to 450 °C. The magnetic properties were probed at room temperature by extraordinary Hall Effect,[29] the magnetic field (up to 12 kOe) being applied perpendicular to the sample plane. For samples with 100% perpendicular remanence, the anisotropy field was determined by applying the external field parallel to the sample plane, with a very small (1°–2°) misorientation in order to ensure a coherent rotation of the magnetization of the Co moments.

Figure 1 shows a series of EHE perpendicular hysteresis loops for different oxidation times from 15 to 60 s. For samples with $t \leq 25$ s, the loops show no hysteresis and zero remanence. Magnetization saturates at high field, showing that the out-of-plane direction is a hard magnetic axis. For $30\ \text{s} \leq t \leq 40$ s, this saturation field considerably decreases to the point where the samples now exhibit a square hysteresis loop with a sharp magnetization reversal. Finally, for $t \geq 45$ s, the loops show no hysteresis and zero remanence. Magnetic measurements with in-plane applied field showed that the single domain state obtained for intermediate oxidation times (between 30 and 40 s) transforms into a multidomain state (for $t \geq 45$ s). The amplitude of the Hall resistance also considerably decreases for the longest oxidation times, as a probable consequence of Co oxidation.[14]

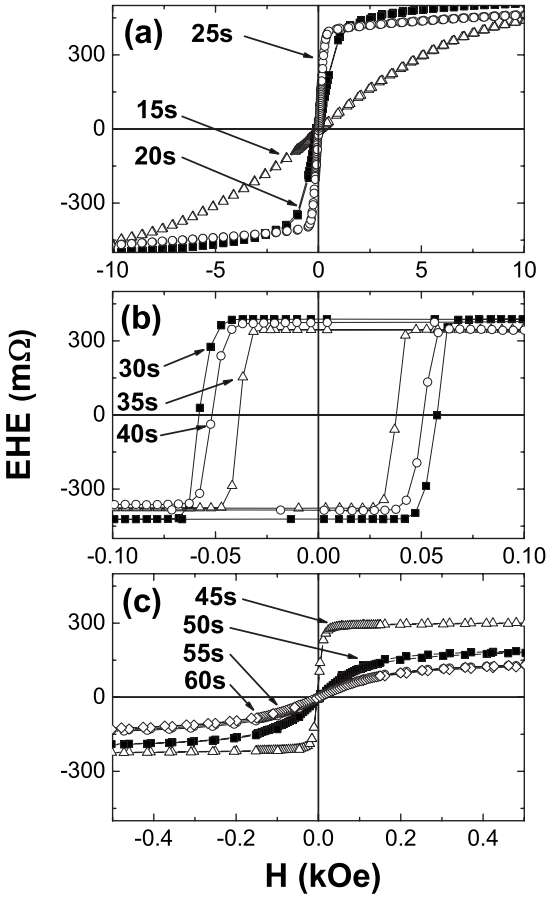

FIG. 1. Variation in the Hall resistance as a function of the applied magnetic field for Pt(3 nm)/Co(0.6 nm)/Al(1.6 nm)/Ox(t) samples, where t is the plasma oxidation time. The field scale is different for the three figures.

The variation of the anisotropy field H_{an} as a function of oxidation time is shown in Fig. 2. It is defined negative when the magnetization lies in the plane of the layer (∥) and positive when it lies out of the plane (⊥). The anisotropy field progressively increases with oxidation time, up to about 8 to

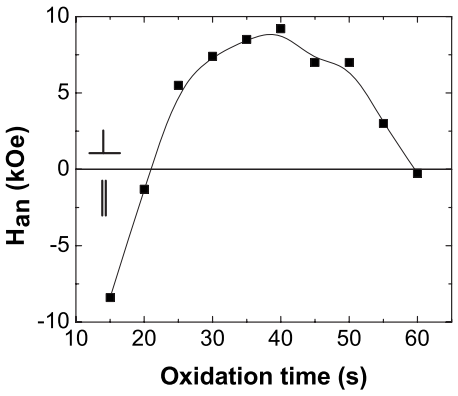

FIG. 2. Anisotropy field of Pt/Co/AlOx samples, measured by EHE, as a function of the oxidation time.

9 kOe for oxidation times of the order of 30 to 40 s, and then decreases for longer oxidation times. The procedure for calculating the anisotropy field will be explained in Sec. III C.

The correlation between the chemical composition of the Co/AlOx interface and the magnetic properties of the Pt/Co/AlOx trilayers has been investigated using x-ray spectroscopy in Ref. 14. In summary, the samples can be divided into three groups, depending on the oxidation time t,

(1) $t \leq 25$ s: the oxygen atoms preferentially diffuse within the Al grain boundaries so that they reach the Co/AlOx interface in an inhomogeneous way, and the oxygen-induced PMA cannot overcome the in-plane shape anisotropy.

(2) 30 s $\leq t \leq 40$ s: a significant amount of oxygen atoms reaches the Co/AlOx interface so that roughly 100% of the interfacial Co-Al bondings are replaced by Co-O ones. Then, the oxygen-induced PMA is maximum and overcomes the in-plane magnetic anisotropy. The magnetization of the Co layer lies out of plane, forming a single domain structure.

(3) 45 s $\leq t$: oxygen atoms penetrate into the Co layer, reducing the exchange coupling between the Co grains, so that the magnetization of the Co layer still lies out of plane but forming a domain structure. For the largest oxidation times, Co strongly oxidizes and the magnetic signal disappears.

III. INFLUENCE OF ANNEALING ON THE MAGNETIC AND TRANSPORT PROPERTIES

We gather now the evolution with annealing temperature T_A of three characteristic quantities: the Hall angle α_H, the nucleation field H_{nuc}, and the anisotropy field H_{an}. The Hall angle is the ratio between the Hall resistivity and the longitudinal resistivity. The longitudinal resistivity has been measured on macroscopic samples, using conventional four-point probes. The nucleation field H_{nuc} is the field at which the magnetization reversal starts and is defined as positive for samples with zero remanence and negative for squared hysteresis loops. For samples with out-of-plane magnetization, the anisotropy field and the nucleation field are determined by using planar and perpendicular external magnetic field, respectively. For samples with in-plane magnetization, both quantities coincide and are determined from Hall measurements with a perpendicular applied field. Note that annealing at 100 °C does not significantly modify the magnetic and chemical properties of the samples, and values measured below that annealing temperature are not reported in the rest of the paper.

A. Hall angle

The Hall angle reveals the capacity of a magnetic system to deviate an electrical current from its initial trajectory. The magnitude of the Hall angle is related to the amplitude of the spin-orbit coupling, to the longitudinal resistivity of the sample, and to the M_z component of the magnetization[30] (i.e., the component perpendicular to the plane of the layers). It must be noted that, for all samples studied here, the longitudinal resistivity varies in a monotonous way upon annealing, and only increases by about 15% after annealing whatever the oxidation time. The different variations reported below thus essentially reflect modifications of the Hall resistivity. Figure 3(a) shows the Hall angle (α_H) measured as a function of the oxidation time for three annealing temperatures (100, 300, and 450 °C). For $T_A = 100$ °C, the Hall angle is only weakly affected by the oxidation time for $t \leq 40$ s. For longer oxidation times ($t \geq 45$ s), most of the decrease in the Hall angle is attributed to the oxidation of the Co layer that induces a decrease in the layer magnetization. Same trends are observed for $T_A = 300$ °C, due to the same effect. After annealing at 300 and 450 °C, the Hall angle is strongly enhanced for short oxidation times (by a factor of almost three) and, for $T_A = 450$ °C, decreases monotonously with increasing oxidation time, contrary to the case of the two other annealing temperatures. Actually, for $T_A = 450$ °C, another mechanism exists: the oxygen atoms are diffusing out of the Co layer[21,31] (see below). This may explain the smaller slope at this annealing temperature.

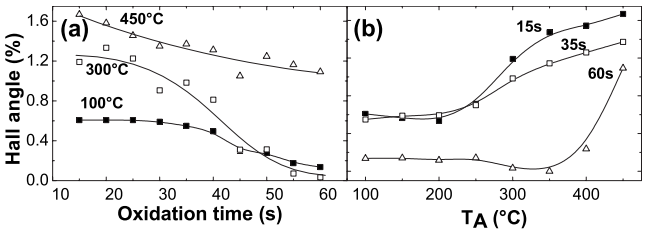

FIG. 3. (a) Hall angle as a function of the oxidation time t for Pt/Co/AlOx samples annealed at 100 °C (filled squares), 300 °C (open squares), and 450 °C (open triangles); (b) Hall angle as a function of the annealing temperature T_A for Pt/Co/AlOx samples oxidized during 15 s (filled squares), 35 s (open squares), and 60 s (open triangles).

Figure 3(b) presents results for three trilayers oxidized during 15, 35, and 60 s as a function of annealing temperature. The Hall angle of the samples oxidized during 15 and 35 s is multiplied by three upon annealing above 250 °C whereas the Hall angle of the sample oxidized during 60 s remains very small (<0.15%) up to 350 °C and only increases after $T_A \geq 400$ °C up to a value close to that of samples oxidized during 15 s and 35 s. This behavior is surprising since at $T_A = 350$ °C, the Hall angle is nearly zero for this sample (hardly no magnetic signal detected). Superconducting quantum interference device (SQUID) measurements show that, for $t = 60$ s, the Co magnetic moment is significantly enhanced after annealing: from a very low value of 175 emu cm^{-3} at $T_A = 150$ °C, the magnetic moment reaches 800 emu cm^{-3} for $T_A = 450$ °C. This moment enhancement can be explained by oxygen diffusion out of the Co layer. The minimum of Hall angle observed at 350 °C for the sample oxidized during 60 s may be explained as follows: in an intermediate stage of the oxygen migration from the Co layer toward the oxide barrier, most of this oxygen is concentrated in the Co grain boundaries. Then the in-plane current flow may have difficulty to propagate in the very thin Co layer because of the highly resistive grain boundaries. As a result, the current mainly flows in the Pt buffer layer resulting in the observed decrease in Hall angle in this regime.

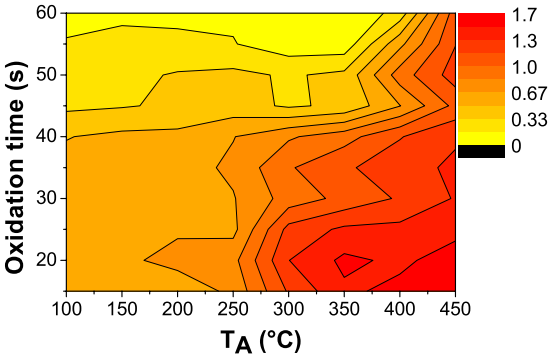

FIG. 4. (Color online) Map of the Hall angle for Pt/Co/AlOx samples, oxidized from 15 to 60 s and annealed from 150 to 450 °C. The color scale is in percent.

Finally, one can note that after annealing at 450 °C, the Hall angle weakly depends on the oxidation time (t).

Figure 4 presents a complete map of the Hall angle as a function of annealing temperature T_A and oxidation time t. A region of significant enhancement of Hall angle appears for small oxidation times and high annealing temperatures.

The behavior of the Hall angle at high annealing temperature is thus attributed to a combination between the Co deoxidation, the related modification of Co/AlOx interface, and the modification of Pt/Co interface (which generally takes place around 250 °C for Pt/Co/Pt trilayers—see Sec. V). For oxidation times of $t=15$ s and $t=30$ s, the diffusion of Pt atoms into the Co layer increases the Hall angle by increasing the spin-orbit scattering within the Co layer. For $t=60$ s, the important oxidation of the Co layer hides this effect. Then, at $T_A=450$ °C the oxygen diffuses out of the Co layer, especially out of the grain boundaries toward the Co/AlOx interface, allowing the enhancement of Co magnetic moment and correlatively of the Hall angle.

B. Nucleation field

The nucleation field, defined above, varies by orders of magnitude as a function of oxidation time and annealing temperature. To conveniently describe these large variations, we adopt the following description:

$$H^* = \log(|H_{\mathrm{nuc}}|), \tag{1}$$

H^* having the sign of H_{nuc}, i.e., being taken as negative for samples with 100% remanence (out-of-plane anisotropy) and positive for samples with 0% remanence (in-plane anisotropy).

Figure 5(a) displays variation in H^* as a function of oxidation time for three annealing temperatures. For $T_A=100$ °C, H^* goes through a negative minimum (100% remanence) for oxidation times around 35 s. For this annealing temperature, only the samples oxidized during $30\ \mathrm{s} \leq t \leq 40$ s show a square hysteresis loop. This minimum of H^* broadens as the annealing temperature increases up to $T_A=450$ °C. For this annealing temperature, all samples exhibit 100% remanence whatever the oxidation time. Figure 5(b) presents the evolution of H^* with annealing temperature for trilayers oxidized during 15, 35, and 60 s. For $t=35$ s, the

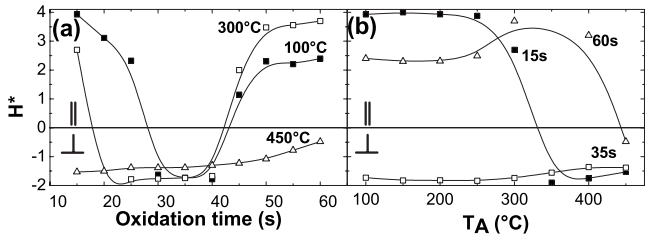

FIG. 5. (a) Nucleation field H^* as a function of the oxidation time t for Pt/Co/AlOx samples annealed at 100, 300, and 450 °C. (b) Nucleation field H^* as a function of annealing temperature T_A for Pt/Co/AlOx samples oxidized during 15, 35, and 60 s. The field scale is logarithmic. Positive values correspond to in-plane magnetization (∥), while negative values indicate out-of-plane magnetization with 100% remanence (⊥).

nucleation field is nearly independent of annealing temperature; the magnetization lies out of plane and the magnetization loop remains square.

However, for the extreme oxidation times, $t=15$ s and $t=60$ s, a strong modification occurs upon annealing. For the underoxidized sample ($t=15$ s), the initial in-plane magnetic anisotropy transforms into an out-of-plane one after annealing above 300 °C. A similar evolution is observed for the overoxidized sample ($t=60$ s). For $T_A=450$ °C, the magnetization goes from an in-plane to an out-of-plane magnetic configuration. This large change in the magnetic state of the under- and overoxidized samples indicates an important modification in the chemical composition of the trilayers during the annealing, as shown in Ref. 21.

Figure 6 presents a map of the variation in H^* as a function of T_A and t. As in Fig. 4, one can distinguish three types of samples: for short oxidation times ($t \leq 25$ s), a crossover of the magnetic anisotropy as a function of the annealing temperature appears around $T_A=300$ °C. For optimally oxidized samples ($t=35$ s), the magnetization loops are essentially independent of the annealing temperature. And finally, for overoxidized samples ($t \geq 45$ s), the magnetization is in plane, with a maximum (positive) nucleation field around 350 °C. However, for higher annealing temperatures ($T_A=450$ °C), these overoxidized samples again display a square magnetization loop. One can again note that, as was

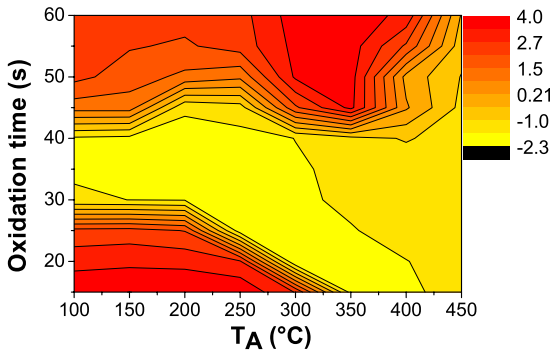

FIG. 6. (Color online) Map of the logarithm of the nucleation field H^* for Pt/Co/AlOx samples, oxidized from 15 to 60 s, and annealed at temperatures from 150 to 450 °C. The color code represents $H^*=\log(|H_{\mathrm{nuc}}|)$.

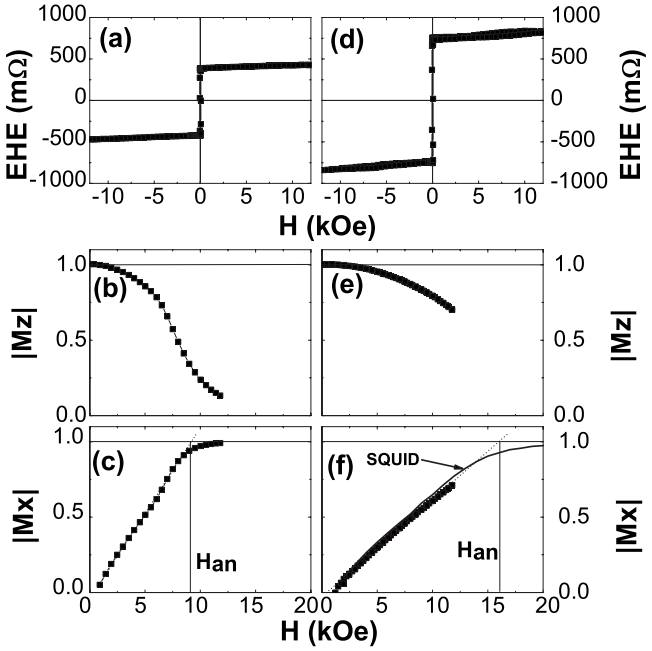

FIG. 7. Variation in the Hall resistance with perpendicular applied field (upper panel), of the M_z component with in-plane applied field (middle panel), and of the correspondent M_x component (bottom panel), obtained for a sample oxidized during $t=35$ s before annealing (on the left), and after annealing at 300 °C (on the right). The SQUID measurement is given by the solid line in (f).

the case of the Hall angle, the nucleation fields of all trilayers tend toward comparable values after high-temperature annealing as shown in Figs. 5(b) and 6.

C. Anisotropy field

The anisotropy field H_{an} is a direct measurement of PMA and is determined from EHE measurements, the external field being applied in the plane of the layers for samples with 100% remanence. The EHE resistance is first normalized to its value at remanence, and M_z then progressively decreases from one to zero with increasing in-plane applied field. We then determine M_x by $M_x(H)=(1-M_z(H)^2)^{1/2}$, and the anisotropy field is calculated from the area above the magnetization curve.

The case of samples with lower anisotropy is slightly more complicated, since, starting from an up-down domain structure in zero field, M_z should in average keep a zero value whatever the applied field. However, the slight misalignment (see Sec. II) between the applied field and the sample plane leads to a nonzero perpendicular component of that applied field. M_z then goes to a maximum before going back to zero at saturation.

This determination of H_{an} is illustrated in Figs. 7(a)–7(c) for a sample oxidized during $t=35$ s before annealing. The calculated M_x component varies almost linearly with applied field, and in that case the saturation field is practically identical to H_{an}.

For samples with anisotropy fields larger than our maximum experimentally available field, 12 kOe [see Fig. 7(e) for instance], the same procedure is followed, but one has now to linearly extrapolate M_x to 1 [Fig. 7(f)].

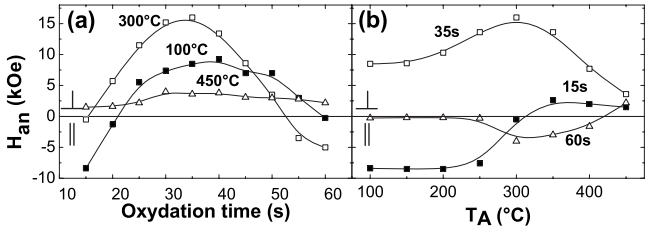

FIG. 8. (a) Anisotropy field as a function of oxidation time for Pt/Co/AlOx samples annealed at 100, 300, and 450 °C. (b) Anisotropy field as a function of annealing temperature for samples oxidized during 15, 35, and 60 s.

To validate this method, we performed a SQUID measurement of the magnetization of that sample [solid line in Fig. 7(f)]. One can see that the extrapolated value of the anisotropy field is very close to the experimental one (within about 15%).

Figure 8(a) shows the variation in the anisotropy field with oxidation time for annealing temperatures of 100, 300, and 450 °C. The anisotropy field goes through a maximum whatever the annealing temperature. The position of this maximum is slightly affected by the annealing temperature, and seems to shift from about 40 s of oxidation time for low annealing temperatures to around 35 s for the highest annealing temperature. The most important feature is that the amplitude of the maximum field is strongly modified by the annealing temperature since it increases by a factor of 2 after annealing at 300 °C. Its amplitude then decreases rapidly for larger annealing temperatures. This confirms the x-ray analysis given in Ref. 21; the anisotropy maximum is obtained for an optimal oxidation of the Co/AlOx interface.

Figure 8(b) shows the variation in H_{an} with annealing temperature measured for samples oxidized during 15, 35, and 60 s. For an oxidation time of 35 s, the maximum field is obtained after 300 °C annealing. Under- and overoxidized samples start evolving at higher temperatures (≥250 °C), and the maximum anisotropy field for $t=15$ s is obtained after 400 °C annealing. For $t=60$ s, the anisotropy field goes through a minimum for $T_A=300-350$ °C, and increases for larger annealing temperatures. One can once again note that, as was the case for the Hall angle [Fig. 3(b)] and for the nucleation field [Fig. 5(b)], the anisotropy field of all trilayers seems nearly independent of the oxidation time after annealing at 450 °C, with a common value of about 2 to 4 kOe.

Figure 9 gathers the anisotropy field measurements performed on these Pt/Co/AlOx samples. In this figure only the positive values of H_{an} are shown. A clear maximum of perpendicular anisotropy is obtained around 30–35 s oxidation times after 300 °C annealing. In that region, SQUID measurements give a value of about 10^3 emu/cm^3 for the saturation magnetization. This leads to a value of the effective anisotropy constant $K_{eff}=H_{an}M_s/2$ of 8×10^6 erg/cm^3 (0.8 MJ/m^3), larger than in most Pt or Pd-based magnetic multilayers.[32]

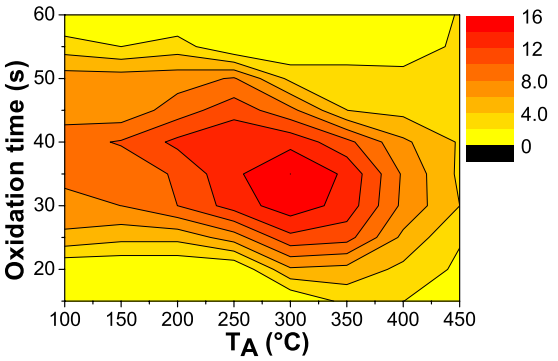

FIG. 9. (Color online) Map of the anisotropy field for Pt/Co/AlOx samples, oxidized from 15 to 60 s, and for annealing temperatures from 150 to 450 °C. The scale is in kilo-oersted and only positive values of the anisotropy field are presented.

IV. INTERPRETATION

For samples with small oxidation times ($t \leq 25$ s), the anisotropy crossover from in-plane to out-of-plane upon annealing (see Fig. 6) is attributed to the thermally induced diffusion of oxygen atoms from the Al_2O_3 barrier toward the Co/AlOx interface. This diffusion is confirmed by x-ray photoemission spectroscopy (XPS) analysis of aluminum oxide within the barrier[21] indicating a significant decrease in the proportion of AlOx/Al upon annealing (decrease by about 10%), together with an increase in the proportion of CoO/Co at the Co/AlOx interface and a homogenization of the interface. The magnetization crossover results in an increased PMA and an enhancement of Hall angle, the former being attributed to oxygen diffusion and the latter to a complex combination of Co-Pt mixing and Co/AlOx and Pt/Co contributions to the interfacial magnetic anisotropy.

For intermediate oxidation times (30 s $\leq t \leq$ 45 s), the annealing temperature only weakly influences the magnetic state of the Co atoms (the magnetization remains out-of-plane without significant modification of the nucleation field—Fig. 6). However, the PMA reaches a maximum for annealing temperatures of 350 °C and the Hall angle slightly increases around this temperature. This behavior can be understood if one considers that, for these oxidation times, the barrier is optimally oxidized. The influence of annealing is to homogenize the barrier, to improve the Co/AlOx interface (decreased roughness), and to modify the Pt/Co interface so that the combination of the two interfacial anisotropies dominates the bulk in-plane shape anisotropy of the Co layer. The underoxidation of the samples oxidized during $t \leq 25$ s does not allow reaching large PMA, certainly due to the insufficient amount of oxygen atoms at the Co/AlOx interface in these samples. Moreover, Co-Pt mixing is probably influenced by the Co/AlOx interface oxidation (the Co layer is only 0.6 nm thick): the presence of CoO bonds seems to rigidify the Pt/Co interface, thus preventing its intermixing.

The overoxidized samples ($t \geq 45$ s) do not seem to be influenced by annealing except for high temperatures, of the order of 400–450 °C. At such high temperatures, oxygen atoms are partially reabsorbed toward the interface (enhancement of the Co magnetic moment for 450 °C annealing).

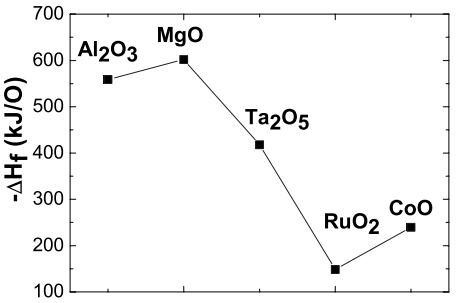

FIG. 10. Enthalpy of formation for Al_2O_3, MgO, Ta_2O_5, RuO_2 and CoO.

Thus, for annealing temperatures less than 400 °C, the oxidation of the Co layer seems to prevent Co-Pt intermixing: there is almost no modification of the magnetic properties of these trilayers. However, above 400 °C, the reabsorption of oxygen allows full deoxidation of the Co layer (and the appearance of a magnetization) and the formation of an optimally oxidized Co/AlOx interface. These two elements give rise to an out-of-plane magnetization in agreement with Lee *et al.*[31] measurements, which show a reabsorption of excess oxygen from the magnetic layer toward the tunnel barrier after 200 °C annealing. However, the origin of the minimum of the Hall angle at annealing temperatures around 350 °C (Fig. 3) remains unclear.

Finally, we noted that all magnetic and transport properties of these trilayers tend to comparable values after annealing at 450 °C, whatever the initial oxidation time. One can imagine a competition between two processes: the oxygen reabsorption and the associated improvement of the Co/AlOx interface on one hand and the Co-Pt mixing on the other hand, itself affected by the presence of CoOx bonds. For such high annealing temperatures, oxygen migration is very important (samples overoxidized at 60 s become magnetic) and the whole Co/AlOx interface tends to be optimally oxidized, so that the magnetic properties of the Co layer no more depend on the initial oxidation time. From these observations, we can infer that the most stable location of the oxygen within these trilayers is right at the Co/AlOx interface where Co-O-Al bonds can be formed.

To conclude, we remind that oxygen-induced PMA has been observed in different Pt(3 nm)/Co(0.6 nm)/M+Ox structures, with M=Al, Mg, Ta, Ru,[14] all of them exhibiting a maximum of magnetic anisotropy for a given oxidation time of the M layer in the as-deposited state. After annealing at 350 °C, an enhancement of perpendicular magnetic anisotropy is observed for MgO and AlOx barriers, while for RuOx and TaOx barriers, the amplitude of EHE signal decreases as well as the PMA compared to the as-deposited state. This behavior can be put in parallel with the enthalpy of formation of these oxides. Figure 10 shows that the enthalpy of formation $-\Delta H_f$ of Al_2O_3 and MgO, is much larger than that of Ta_2O_5, RuO_2, and CoO. Furthermore, the ruthenium oxide enthalpy of formation is smaller than that of CoO, thus favoring the diffusion of oxygen within the Co layer. This explains why Al_2O_3 and MgO barriers are more thermally stable than Ta_2O_5 and RuO_2 barriers and that annealing has a different influence on these different barriers.

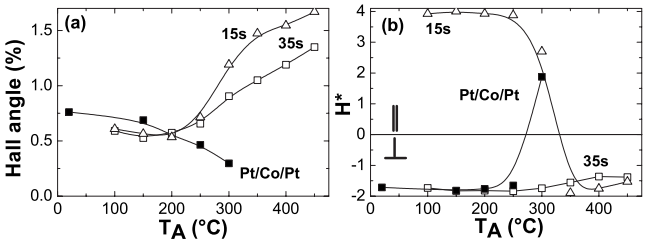

FIG. 11. (a) Hall angle and (b) nucleation field—logarithmic scale—for Pt/Co/AlOx samples oxidized during $t=15$ s (open triangles) and $t=35$ s (open squares) and for a Pt/Co/Pt sample (filled squares).

V. COMPARISON WITH Pt/Co/Pt TRILAYERS

The comparison between Pt/Co/Pt and Pt/Co/AlOx trilayers is instructive, in terms of both perpendicular anisotropy and thermal stability. Pt/Co/Pt systems have been extensively studied for their PMA and their applications in magneto-optic recording.[33] However, Pt/Co/AlOx trilayers exhibit more interesting magnetic (PMA) and electrical (Hall angle) properties than Pt/Co/Pt trilayers, together with a much better thermal stability. Figure 11(a) displays the dependence of the Hall angle as a function of annealing temperature for Pt(3 nm)/Co(0.6 nm)/Pt(2 nm) samples and Pt(3 nm)/Co(0.6 nm)/Al(1.6 nm)+Ox ones oxidized during $t=15$ s and $t=35$ s.

The Hall angle of the as-deposited Pt/Co/Pt trilayer is slightly larger than in as-deposited Pt/Co/AlOx trilayers. However, it decreases monotonously as annealing temperature increases. On the contrary, as we previously showed, the Hall angle of Pt/Co/AlOx samples continuously increases with annealing temperature in the range 200–400 °C and can reach, depending on the oxidation time and annealing temperature, values of the order of 2%. In contrast, Pt/Co/Pt trilayers become nonmagnetic around $T_A=350$ °C, which confirms the "rigidifying" effect of the Co/AlOx interface on the Pt/Co interface.

Figure 11(b) shows the evolution of the nucleation field with annealing temperature for both structures. We observe that beyond 250 °C, the magnetization loop of Pt/Co/Pt shows no more hysteresis and the magnetization is no more out of plane, whereas that of Pt/Co/AlOx structures is out of plane whatever the oxidation time for annealing temperatures above 300 °C.

The anisotropy field of Pt/Co/Pt does not exceed 5 kOe, whereas Pt/Co/AlOx samples can present anisotropy fields up to 16 kOe (for $t=35$ s and $T_A=350$ °C). It clearly appears that Pt/Co/AlOx have major advantages compared to Pt/Co/Pt structures. The use of magnetic layers with perpendicular magnetization in spin valves,[34] magnetic tunnel junctions,[27] and EHE sensors requires good temperature stability, a property that Pt/Co/Pt multilayers cannot achieve because of Co/Pt intermixing.

VI. CONCLUSION

The influence of annealing temperature has been investigated in Pt/Co/AlOx trilayers, for various plasma oxidation times. The magnetic and electrical properties are strongly modified by thermal diffusion of oxygen toward the Co/AlOx interface.

Although some peculiar features of these materials are still not fully understood, it seems that the largest PMA energies are reached as soon as all Co-Al bonds are replaced by Co-O ones, depending on either oxidation time or annealing. Preliminary x-ray reflectivity measurements seem to confirm this interpretation.[35]

At high annealing temperatures, the magnetic properties converge toward comparable values (in terms of both Hall angle, coercive field, or anisotropy field, whatever the initial oxidation time). Based on former studies,[14,21] this is interpreted as a combination between oxygen diffusion and chemical modification of Co/AlOx and Pt/Co interfaces upon annealing. This convergence of the magnetic properties after high-temperature annealing (450 °C) seems to indicate that the most stable location of oxygen in these Pt/Co/AlOx trilayers is right at the Co/AlOx interface where Co-O-Al bonds can be formed.

These structures show much better perpendicular anisotropy properties than classical Pt/Co/Pt trilayers, and have been already used for current-induced domain-wall motion studies, revealing improved characteristics compared to Pt/Co/Pt trilayers.[36] They are also considerably more thermally stable, probably because of the rigidification of the Pt/Co interface induced by the presence of oxygen atoms at the Co/AlOx interface.

From a practical point of view, in these Pt/Co/AlOx trilayers, it is possible to tune the magnetic properties at will, and thus obtain, by varying the oxidation conditions (time and annealing temperature), either materials with a large Hall angle (almost 2%), or with a very small coercive field (a few Oersted), or with very strong perpendicular anisotropy (16 kOe).

ACKNOWLEDGMENTS

The authors acknowledge very fruitful discussions with C. Lacroix, A. Bergmann, and M. Chshiev. A.M. acknowledges partial financial support from NSF (Grant No. DMR-0704182) and DOE (Grant No. DE-FG02-06ER4630).

[1] M. Julliere, Phys. Lett. **54A**, 225 (1975).
[2] S. Mao, J. Nanosci. Nanotechnol. **7**, 1 (2007).
[3] Y. Zheng, Y. Wu, K. Li, J. Qiu, G. Han, Z. Guo, P. Luo, L. An, Z. Liu, L. Wang, S. G. Tan, B. Zong, and B. Liu, J. Nanosci. Nanotechnol. **7**, 117 (2007).
[4] J. S. Moodera, L. R. Kinder, T. M. Wong, and R. Meservey, Phys. Rev. Lett. **74**, 3273 (1995).
[5] S. S. P. Parkin, C. Kaiser, A. Panchula, P. M. Rice, B. Hughes,

M. Samant, and S.-H. Yang, Nature Mater. **3**, 862 (2004); S. Yuasa, T. Nagahama, A. Fukushima, Y. Suzuki, and K. Ando, *ibid.* **3**, 868 (2004).
[6] E. Y. Tsymbal, O. N. Mryasov, and P. R. LeClair, J. Phys.: Condens. Matter **15**, R109 (2003).
[7] R. C. Sousa, J. J. Sun, V. Soares, P. P. Freitas, A. Kling, M. F. da Silva, and J. C. Soares, Appl. Phys. Lett. **73**, 3288 (1998).
[8] J. S. Bae, K. H. Shin, T. D. Lee, and H. M. Lee, Appl. Phys. Lett. **80**, 1168 (2002).
[9] Y. Wang, Z. M. Zeng, X. F. Han, X. G. Zhang, X. C. Sun, and Z. Zhang, Phys. Rev. B **75**, 214424 (2007).
[10] B. S. Mun, J. C. Moon, S. W. Hong, K. S. Kang, K. Kim, T. W. Kim, and H. L. Ju, J. Appl. Phys. **99**, 08E506 (2006).
[11] F. F. Li, R. Sharif, L. X. Jiang, X. Q. Zhang, X. F. Han, Y. Wang, and Z. Zhang, J. Appl. Phys. **98**, 113710 (2005).
[12] S. Ikeda, J. Hayakawa, Y. M. Lee, R. Sasaki, T. Meguro, F. Matsukura, and H. Ohno, Jpn. J. Appl. Phys., Part 2 **44**, L1442 (2005); S. Ikeda, J. Hayakawa, Y. Ashizama, Y. M. Lee, K. Miura, H. Hasegawa, M. Tsunoda, F. Matsukura, and H. Ohno, Appl. Phys. Lett. **93**, 082508 (2008).
[13] A. N. Chiaramonti, D. K. Schreiber, W. F. Egelhoff, D. N. Seidman, and A. K. Petford-Long, Appl. Phys. Lett. **93**, 103113 (2008).
[14] A. Manchon, S. Pizzini, J. Vogel, V. Uhlir, L. Lombard, C. Ducruet, S. Auffret, B. Rodmacq, B. Dieny, M. Hochstrasser, and G. Panaccione, J. Appl. Phys. **103**, 07A912 (2008).
[15] D. Weller, Y. Wu, J. Stohr, M. G. Samant, B. D. Hermsmeier, and C. Chappert, Phys. Rev. B **49**, 12888 (1994).
[16] N. Nakajima, T. Koide, T. Shidara, H. Miyauchi, H. Fukutani, A. Fujimori, K. Iio, T. Katayama, M. Nyvlt, and Y. Suzuki, Phys. Rev. Lett. **81**, 5229 (1998).
[17] G. H. O. Daalderop, P. J. Kelly, and M. F. H. Schuurmans, Phys. Rev. B **50**, 9989 (1994).
[18] P. Bruno, Phys. Rev. B **39**, 865 (1989).
[19] S. Monso, B. Rodmacq, S. Auffret, G. Casali, F. Fettar, B. Gilles, B. Dieny, and P. Boyer, Appl. Phys. Lett. **80**, 4157 (2002).
[20] D. Lacour, M. Hehn, M. Alnot, F. Montaigne, F. Greullet, G. Lengaigne, O. Lenoble, S. Robert, and A. Schuhl, Appl. Phys. Lett. **90**, 192506 (2007).
[21] A. Manchon, S. Pizzini, J. Vogel, V. Uhlir, L. Lombard, C. Ducruet, S. Auffret, B. Rodmacq, B. Dieny, M. Hochstrasser, and G. Panaccione, J. Magn. Magn. Mater. **320**, 1889 (2008).
[22] N. Nishimura, T. Hirai, A. Koganei, T. Ikeda, K. Okano, Y. Sekiguchi, and Y. Osada, J. Appl. Phys. **91**, 5246 (2002).
[23] G. Kim, Y. Sakuraba, M. Oogane, Y. Ando, and T. Miyazaki, Appl. Phys. Lett. **92**, 172502 (2008).
[24] M. Nakayama, T. Kai, N. Shimomura, M. Amano, E. Kitagawa, T. Nagase, M. Yoshikawa, T. Kishi, S. Ikegawa, and H. Yoda, J. Appl. Phys. **103**, 07A710 (2008); H. Ohmori, T. Hatori, and S. Nakagawa, *ibid.* **103**, 07A911 (2008).
[25] D. Lim, S. Kim and S.-R. Lee, J. Appl. Phys. **97**, 10C902 (2005).
[26] J.-H. Park, C. Park, T. Jeong, M. T. Moneck, N. T. Nufer, and J.-G. Zhu, J. Appl. Phys. **103**, 07A917 (2008).
[27] C. Ducruet, B. Carvello, B. Rodmacq, S. Auffret, G. Gaudin, and B. Dieny, J. Appl. Phys. **103**, 07A918 (2008).
[28] L. Gao, X. Jiang, S.-H. Yang, J. D. Burton, E. Y. Tsymbal, and S. S. P. Parkin, Phys. Rev. Lett. **99**, 226602 (2007); A. N. Chantis, K. D. Belashchenko, E. Y. Tsymbal, and M. van Schilfgaarde, *ibid.* **98**, 046601 (2007).
[29] A. Gerber, A. Milner, M. Karpovsky, B. Lemke, H.-U. Habermeier, J. Tuaillon-Combes, M. Négrier, O. Boisron, P. Mélinon, and A. Perez, J. Magn. Magn. Mater. **242-245**, 90 (2002).
[30] S. Zhang, Phys. Rev. B **51**, 3632 (1995).
[31] J. H. Lee, D. H. Im, C. S. Yoon, C. K. Kim, Y. Ando, H. Kubota, and T. Miyazaki, J. Appl. Phys. **94**, 7778 (2003).
[32] V. W. Guo, B. Lu, X. Wu, G. Ju, B. Valcu, and D. Weller, J. Appl. Phys. **99**, 08E918 (2006).
[33] P. Poulopoulos, M. Angelakeris, E. Th. Papaioannou, N. K. Flevaris, D. Niarchos, M. Nyvlt, V. Prosser, and S. Visnovsky, J. Appl. Phys. **94**, 7662 (2003).
[34] D. Houssameddine, U. Ebels, B. Delaët, B. Rodmacq, I. Firastrau, F. Ponthenier, M. Brunet, C. Thirion, J.-P. Michel, L. Prejbeanu-Buda, M.-C. Cyrille, O. Redon, and B. Dieny, Nature Mater. **6**, 447 (2007).
[35] H. Garad, F. Fettar, L. Ortega, B. Rodmacq, S. Auffret, and B. Dieny (unpublished).
[36] I. M. Miron, P.-J. Zermatten, G. Gaudin, S. Auffret, B. Rodmacq, and A. Schuhl, arXiv:0810.4633 (unpublished).